



# High-temperature synthesis and unknown properties of $M_3Cr_4(PO_4)_6$ , where $M = Zn$ or $Mg$ and a new solid solution $Zn_{1.5}Mg_{1.5}Cr_4(PO_4)_6$

Anna Blonska-Tabero<sup>1</sup> · Monika Bosacka<sup>1</sup> · Elzbieta Filipek<sup>1</sup> · Mateusz Piz<sup>1</sup> · Pawel Kochmanski<sup>2</sup>

Received: 12 June 2019 / Accepted: 3 November 2019 / Published online: 19 November 2019  
© Akadémiai Kiadó, Budapest, Hungary 2019

## Abstract

For the first time, double phosphates(V)  $Zn_3Cr_4(PO_4)_6$  and  $Mg_3Cr_4(PO_4)_6$  were synthesized by non-waste solid-state reaction, performed in the temperature range 350–1150 °C. The change in the phase composition of samples during the synthesis, depending on the heating temperature, was examined using the XRD method. The results of the DTA measurements enabled both the correct selection of the heating temperatures of the samples and the determination of the thermal stability of the phases obtained.  $Zn_3Cr_4(PO_4)_6$  and  $Mg_3Cr_4(PO_4)_6$  have relatively high thermal stability in air, i.e. they melt incongruently at 1340 °C and about 1450 °C, respectively. Crystallites of the obtained double phosphates, observed by SEM method, are similar in shape, when their sizes are of the order of 0.5–6 μm. IR spectra of both double phosphates are presented. A new solid solution of the formula  $Zn_{1.5}Mg_{1.5}Cr_4(PO_4)_6$  was also obtained. It is stable in air up to 1412 °C. The energy gaps of  $Zn_3Cr_4(PO_4)_6$ ,  $Mg_3Cr_4(PO_4)_6$  and  $Zn_{1.5}Mg_{1.5}Cr_4(PO_4)_6$  are 4.00, 3.60 and 3.75 eV, respectively, as estimated from their UV–Vis DR spectra. The colour of all phases expressed in the coordinates of CIE  $L^*C^*h^*$  colour space is very similar, and according to the RAL system, it can be described as boulder brown. All the obtained phases are good candidates to be as inorganic pigments.

**Keywords** Chromium magnesium zinc phosphates · High-temperature reactions · DTA · XRD · SEM · UV–Vis (DRS)

## Introduction

It is known from the literature that phosphates(V) of di- and trivalent metals have been for many years the objects of intensive studies, because they can be applied as inorganic pigments, as components of catalysts of different chemical processes or as electrode materials [1–6]. Taking into account this information, it can be assumed that also double phosphates(V), i.e. containing mixed di- and trivalent cation, can be very important for designing of new materials to be applied in different areas of technology. However, physicochemical properties of most of the

double phosphates(V) have been so far investigated only in a fragmentary way, which makes it impossible to know their potential possibilities.

Merely two papers [7, 8] were found referring to double phosphates(V)  $Zn_3Cr_4(PO_4)_6$  and  $Mg_3Cr_4(PO_4)_6$ ; what is more, both concern only the structures of these compounds. The above-mentioned compounds are the members of the  $Fe_3^{2+}Fe_4^{3+}(PO_4)_6$  structure type family [7, 8], comprising a large number of phases, including not only phosphates, but also vanadates, molybdates and arsenates [9]. For example, the solid solution  $Mn_{3-x}Mg_xFe_4(PO_4)_6$  ( $0 \leq x \leq 3$ ) has the above structure and this solution produces interesting brown colourations in ceramic glazes [9]. On the other hand, phosphates are also a good alternative for the withdrawn anticorrosive chromates(VI). The best example is the conventionally used zinc orthophosphate(V) with its toxicity several times lower than that of chromates(VI) [3]. Unfortunately, an urgent problem becomes the gradual introduction of too much zinc ions to the natural environment. As a result, the other phosphates are studied in order to find new environmentally friendly pigments [3]. It has been confirmed that

✉ Anna Blonska-Tabero  
abtab@zut.edu.pl

<sup>1</sup> Department of Inorganic and Analytical Chemistry, Faculty of Chemical Technology and Engineering, West Pomeranian University of Technology, Szczecin, Al. Piastow 42, 71-065 Szczecin, Poland

<sup>2</sup> Faculty of Mechanical Engineering and Mechatronics, West Pomeranian University of Technology, Szczecin, Al. Piastow 19, 70-310 Szczecin, Poland

inter alia chromium(III) phosphates(V) show high anticorrosion efficiency [3].

In the light of the above literature data,  $\text{Zn}_3\text{Cr}_4(\text{PO}_4)_6$  and  $\text{Mg}_3\text{Cr}_4(\text{PO}_4)_6$ , i.e. double phosphates containing trivalent chromium and divalent magnesium or zinc, can be interesting for designing of new inorganic pigments. As mentioned above, except for the structure, there is no information about  $\text{Zn}_3\text{Cr}_4(\text{PO}_4)_6$  and  $\text{Mg}_3\text{Cr}_4(\text{PO}_4)_6$ . Therefore, the aim of the presented work was to synthesize and to investigate some of their physicochemical properties, including their thermal stability, size of grains and colour (very important for potential pigments), but also their infrared spectra and results of spectrophotometric measurements, which have not been presented until now. In our study for the first time,  $\text{Zn}_3\text{Cr}_4(\text{PO}_4)_6$  and  $\text{Mg}_3\text{Cr}_4(\text{PO}_4)_6$  were obtained by solid-state reaction method. This method, in comparison with “wet” method and chemical transport applied by the authors of [7], is admittedly time-consuming, but non-waste and relatively simple. The additional aim of the work was to find out whether  $\text{Zn}_3\text{Cr}_4(\text{PO}_4)_6$  and  $\text{Mg}_3\text{Cr}_4(\text{PO}_4)_6$  form a solid solution. Such a possibility is very important, because it enables partial replacement of zinc ions with more environmentally friendly ones, e.g. magnesium ions, and modification of physicochemical properties of the obtained potential pigments. So, if  $\text{Zn}_3\text{Cr}_4(\text{PO}_4)_6$  shows high anticorrosion efficiency (as  $\text{Zn}_3(\text{PO}_4)_2$ ), a necessary reduction in zinc content could be achieved.

## Experimental

The initial reagents used in the study were:  $3\text{MgCO}_3 \cdot \text{Mg}(\text{OH})_2 \cdot 3\text{H}_2\text{O}$  (p.a., POCh, Poland),  $\text{ZnO}$  (99.9%, Sigma-Aldrich, USA),  $(\text{NH}_4)_2\text{HPO}_4$  (p.a., Chempur, Poland),  $\text{Cr}_2\text{O}_3$  (99%, Acros Organics, Germany). Syntheses were conducted by the conventional method of calcining samples described inter alia in the papers [10–13]. Stoichiometric mixtures of reacting substances were homogenized by grinding in an automated agate mortar, and then, they were heated in air atmosphere in several stages. After each heating stage, the samples were gradually cooled down in the furnace to room temperature, ground and examined by XRD method with respect to their composition. This procedure was repeated until the monophasic samples were obtained. To avoid the melting of the samples, the maximum temperature of their heating was a few ten degrees lower than their melting points found from DTA curves. The exceptions were the first stages of syntheses, when oxide precursors were used. In such cases, the temperature in the furnace was gradually increased from 350 to 650 °C, which was applied mainly to remove  $\text{NH}_3$ ,  $\text{CO}_2$  or steam as gas products of the occurring reactions [10, 14]. After gas removal, the samples were heated in the form of pastilles.

The XRD patterns of samples were recorded with the aid of the Empyrean II diffractometer (PANalytical, Netherlands) with  $\text{CuK}_\alpha$  radiation. The identification of phases, present in the samples, was carried out on the basis of their XRD characteristics contained in the PDF cards.

The DTA measurements were performed in air atmosphere using an instrument of a SDT 2960 type (TA Instruments, USA). Samples of ~ 25 mg each were heated in corundum crucibles from room temperature up to ~ 1450 °C at a heating rate of 10 °C  $\text{min}^{-1}$ . The investigations up to ~ 1500 °C were conducted using an optical pyrometer (Raytek, model RAYMMIMHSF2V, Germany).

The densities of the obtained phases were determined with the help of an Ultrapyc 1200e ultrapycnometer (Quantachrome Instruments, USA); argon (5 N purity) was used as a pycnometric gas. The measurements were performed in five repetitions using ~ 2 g of each sample for the test.

The IR measurements (the Specord M 80 spectrometer, Carl Zeiss, Germany) were conducted applying the technique of pressing pastilles of the sample with KBr at the ratio 1:300 by mass.

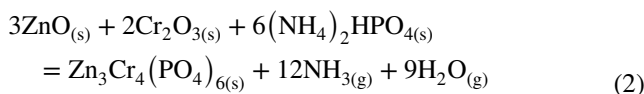
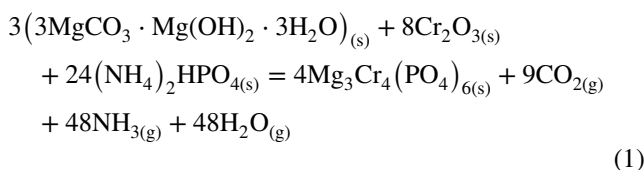
The shape and size of the obtained crystallites were observed by means of SEM method (FE-SEM Hitachi SU-70 microscope).

The UV–Vis diffuse reflectance spectra of obtained phases were recorded using a UV–Vis spectrometer V-670 (JASCO, Japan) equipped with a reflecting attachment for solid-state investigation (integrating sphere attachment with horizontal sample platform PIV-756/(PIN-757)). The spectra were recorded in the wavelength region of 200–800 nm at room temperature using barium sulphate for reference. The spectral bandwidth was 5 nm.

## Results and discussion

### Solid-state synthesis and XRD characterization

$\text{Mg}_3\text{Cr}_4(\text{PO}_4)_6$  and  $\text{Zn}_3\text{Cr}_4(\text{PO}_4)_6$  were obtained according to the following summary reactions:

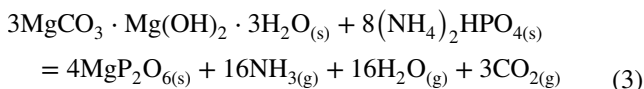


Stoichiometric mixtures of reagents were heated in the following stages:

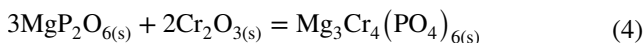
- Synthesis of  $Mg_3Cr_4(PO_4)_6$ : 350 °C(8 h) → 550 °C(8 h) → 650 °C(12 h) + 750 °C(12 h) + 1000 °C(12 h) + 1050 °C(12 h) + 1100 °C(12 h) × 3 + 1150 °C(12 h)
- Synthesis of  $Zn_3Cr_4(PO_4)_6$ : 350 °C(8 h) → 550 °C(8 h) → 650 °C(12 h) + 750 °C(12 h) + 800 °C(12 h) + 900 °C(12 h) + 950 °C(12 h) + 1000 °C(12 h) + 1100 °C(12 h) + 1150 °C(12 h)

The change in the phase composition of samples during the synthesis, depending on the heating temperature, is presented in Table 1.

The data show that in the first stage of the synthesis of  $Mg_3Cr_4(PO_4)_6$  compound, in the temperature range from 350 to 650 °C, a reaction occurs to form  $MgP_2O_6$ :



The synthesis of  $Mg_3Cr_4(PO_4)_6$  began at a temperature of about 750 °C, at which magnesium metaphosphate(V) reacts with chromium(III) oxide, present in the reagent mixture, according to the reaction:

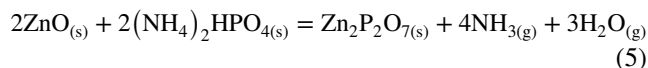


After subsequent heating stages of the sample in the temperature range of 1000–1100 °C, three compounds were identified in it, whereas the  $Mg_3Cr_4(PO_4)_6$  content gradually increased with a decreasing content of  $MgP_2O_6$  and  $Cr_2O_3$ . A monophasic sample containing  $Mg_3Cr_4(PO_4)_6$  was obtained at 1150 °C.

As can be seen from the data presented in Table 1, after the first two stages of  $Zn_3Cr_4(PO_4)_6$  synthesis, zinc

pyrophosphate(V) and unreacted chromium(III) oxide were identified in the sample. The diffractograms contained also a set of lines that could not be assigned to any of the known phases forming in the side systems of the  $ZnO-P_2O_5-Cr_2O_3$  system. It was therefore concluded that the set of lines is related to the presence of a previously unknown phase (marked as X), which forms as an intermediate product during synthesis. Research aimed at determining the composition of phase X will be continued.

Thus, in the case of the synthesis of  $Zn_3Cr_4(PO_4)_6$ , two reactions take place in parallel in the temperature range of 350–750 °C. The first of these leads to the formation of  $Zn_2P_2O_7$  according to the equation:



On the basis of the phase composition of this sample, it can be additionally thought that  $Zn_2P_2O_7$  reacts with the chromium(III) oxide and  $(NH_4)_2HPO_4$ , present in the initial mixture, to form the X phase.

Under the conditions of the experiment, the synthesis of  $Zn_3Cr_4(PO_4)_6$  began at a temperature of about 800 °C. With the increase in temperature in the subsequent stages of heating, the content of  $Cr_2O_3$ ,  $Zn_2P_2O_7$  and X phase in the sample decreased gradually and the  $Zn_3Cr_4(PO_4)_6$  content increased simultaneously. Zinc pyrophosphate(V) reacted completely at 950 °C. Further steps of the synthesis performed in the temperature range 1000–1150 °C indicate that compound X reacts with  $Cr_2O_3$  to form  $Zn_3Cr_4(PO_4)_6$ . Monophasic sample, containing only  $Zn_3Cr_4(PO_4)_6$ , was obtained at 1150 °C.

The diffraction patterns, taken after the last heating stage of both samples, were consistent with the XRD characteristics of  $Mg_3Cr_4(PO_4)_6$  and  $Zn_3Cr_4(PO_4)_6$ , respectively, contained in the PDF cards No. 86-1997 and 86-1996.

**Table 1** Phase composition of the samples after subsequent stages of their heating

Synthesis of $Mg_3Cr_4(PO_4)_6$		Synthesis of $Zn_3Cr_4(PO_4)_6$	
Heating temperature	Phases detected	Heating temperature	Phases detected
350 °C (8 h) → 550 °C(8 h) → 650 °C (12 h)	$MgP_2O_6$ , $Cr_2O_3$	350 °C (8 h) → 550 °C (8 h) → 650 °C (12 h)	$Cr_2O_3$ , $Zn_2P_2O_7$ , X phase
750 °C (12 h)	$MgP_2O_6$ , $Cr_2O_3$ , $Mg_3Cr_4(PO_4)_6^*$	750 °C(12 h)	
1000 °C (12 h)	$Mg_3Cr_4(PO_4)_6$ , $MgP_2O_6$ , $Cr_2O_3$	800 °C(12 h)	$Zn_3Cr_4(PO_4)_6$ , $Cr_2O_3$ , $Zn_2P_2O_7$ , X phase
1050 °C (12 h)		900 °C(12 h)	
1100 °C (12 h)		950 °C(12 h)	$Zn_3Cr_4(PO_4)_6$ , $Cr_2O_3$ , X phase
1100 °C (12 h)		1000 °C(12 h)	
1100 °C (12 h)	$Mg_3Cr_4(PO_4)_6$ , $MgP_2O_6^*$ , $Cr_2O_3^*$	1100 °C(12 h)	$Zn_3Cr_4(PO_4)_6$ , $Cr_2O_3^*$ , X phase*
1150 °C (12 h)	$Mg_3Cr_4(PO_4)_6$	1150 °C(12 h)	$Zn_3Cr_4(PO_4)_6$

\*A small amount

## Thermal stability

Thermal stability up to 1100 °C enables the use of the obtained compounds for colouring of commercially available middle-temperature ceramic glazes. To determine thermal stability of  $\text{Zn}_3\text{Cr}_4(\text{PO}_4)_6$  and  $\text{Mg}_3\text{Cr}_4(\text{PO}_4)_6$ , both compounds were studied by DTA method. In the DTA curve of  $\text{Zn}_3\text{Cr}_4(\text{PO}_4)_6$  (Fig. 1), only one endothermic effect was recorded, with onset temperature of 1340 °C. In order to determine the type of the transformation that the effect is due to, a sample of  $\text{Zn}_3\text{Cr}_4(\text{PO}_4)_6$  was heated for 1 h at 1360 °C (i.e. at the temperature of the maximum of this effect), and then, it was rapidly cooled to room temperature, ground and subjected to XRD study. On removal from the furnace at 1360 °C, the liquid was observed, so the recorded endothermic effect is connected with melting of  $\text{Zn}_3\text{Cr}_4(\text{PO}_4)_6$ . In the “frozen” sample, two solid phases were identified, i.e.  $\alpha\text{-CrPO}_4$  and  $\text{Cr}_2\text{O}_3$  (stable up to 1450 °C and 2335 °C, respectively [15, 16]).  $\alpha\text{-Zn}_2\text{P}_2\text{O}_7$  was also identified, but taking into account its melting point (i.e. about 1000 °C), it can be concluded that zinc pyrophosphate(V) crystallized from the liquid. The obtained results point to incongruent melting of  $\text{Zn}_3\text{Cr}_4(\text{PO}_4)_6$ .

In the DTA curve of  $\text{Mg}_3\text{Cr}_4(\text{PO}_4)_6$ , no thermal effects were recorded, so it was concluded that this compound undergoes melting or decomposition at temperature very close or higher than 1450 °C. To establish its thermal stability, the sample containing  $\text{Mg}_3\text{Cr}_4(\text{PO}_4)_6$  was heated in air atmosphere in a horizontal tube furnace equipped with an optical pyrometer. According to the result of the performed experiment, it was estimated that the compound under study is stable in air up to ~1450 °C. XRD analysis, performed for the sample after experiment, indicates that  $\text{Mg}_3\text{Cr}_4(\text{PO}_4)_6$  melts incongruently with the formation of

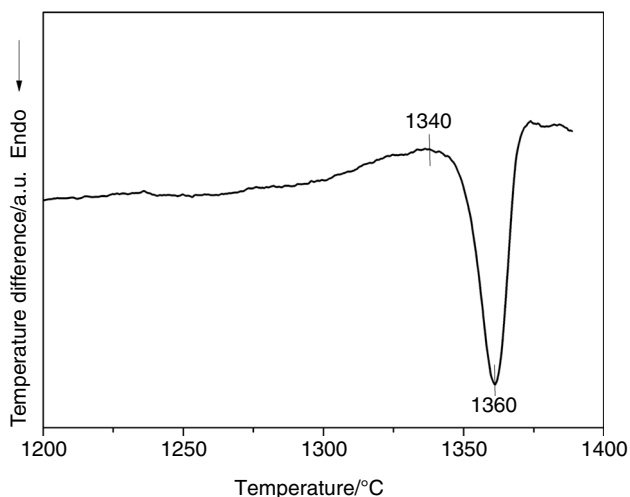


Fig. 1 Fragment of DTA curve of  $\text{Zn}_3\text{Cr}_4(\text{PO}_4)_6$

$\text{Cr}_2\text{O}_3$ . Magnesium pyrophosphate(V) was also identified in the sample.  $\text{Mg}_2\text{P}_2\text{O}_7$  with its melting point at 1395 °C [2], like  $\text{Zn}_2\text{P}_2\text{O}_7$ , most likely crystallized from the liquid.

## SEM investigation

Sizes of grains rank among fundamental properties of solids when applying them, for example, as inorganic pigments, because they determine the intensity of colour and dispersion of pigment in the binding system applied. The recommended mean sizes of inorganic pigment grains depend on the particular application, although in general they lie in the range 0.01–10  $\mu\text{m}$  [17]. To gain the information about the obtained compounds on the microscale, their characterization by SEM method was made. The grains of  $\text{Zn}_3\text{Cr}_4(\text{PO}_4)_6$  and  $\text{Mg}_3\text{Cr}_4(\text{PO}_4)_6$  (Figs. 2, 3) are similar in their shape, and both are much differentiated in sizes. The sizes of the larger crystallites are of the order of 6  $\mu\text{m}$  (for  $\text{Zn}_3\text{Cr}_4(\text{PO}_4)_6$ ) or 4  $\mu\text{m}$  (for  $\text{Mg}_3\text{Cr}_4(\text{PO}_4)_6$ ), whereas the sizes of the smaller crystallites do not often exceed 1  $\mu\text{m}$  or 0.5  $\mu\text{m}$  for  $\text{Zn}_3\text{Cr}_4(\text{PO}_4)_6$  and  $\text{Mg}_3\text{Cr}_4(\text{PO}_4)_6$ , respectively.

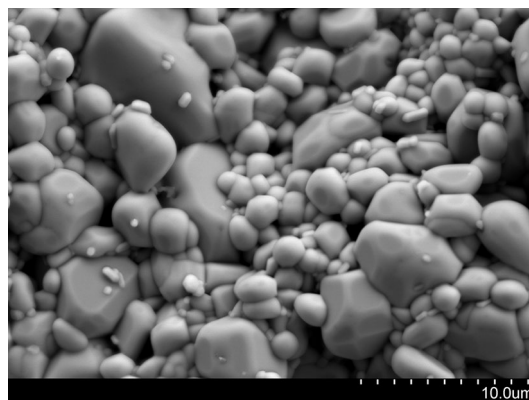


Fig. 2 SEM image of  $\text{Zn}_3\text{Cr}_4(\text{PO}_4)_6$

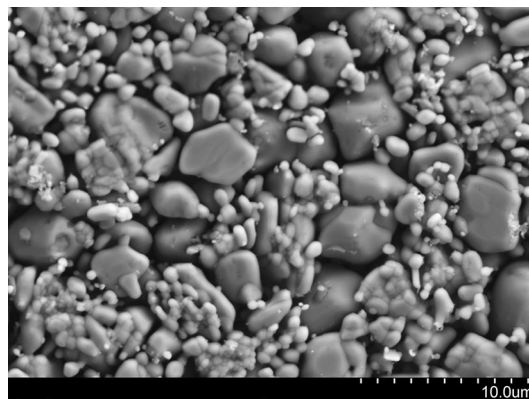


Fig. 3 SEM image of  $\text{Mg}_3\text{Cr}_4(\text{PO}_4)_6$

It can be therefore concluded that the recommended mean grain size was attained for the prepared samples.

### Infrared spectra

Figure 4 presents the IR spectra of  $Zn_3Cr_4(PO_4)_6$  and  $Mg_3Cr_4(PO_4)_6$  in the wave number range  $1350\text{--}300\text{ cm}^{-1}$ . The structures of both double phosphates are known [7, 8], so probable attribution of the recorded absorption bands to the vibrations in concrete polyhedra can be made in the light of the literature data. As the obtained compounds are isostructural, both spectra exhibit much similarity. Three regions of absorption bands can be distinguished in these spectra. The first one between  $1350$  and  $700\text{ cm}^{-1}$  exhibits absorption maxima at  $1220$ ,  $1155$ ,  $1110$ ,  $1020$ ,  $960$ ,  $925\text{ cm}^{-1}$ . This wide band is characteristic for orthophosphate ions [18]. In this wave number range, the absorption is assigned to the stretching symmetric and asymmetric vibration of P–O bonds in the  $PO_4$  tetrahedra [18–23]. The second absorption band in the wavenumber range  $700\text{--}490\text{ cm}^{-1}$  probably comes from the stretching vibrations of M–O bonds in the  $MO_5$  ( $M = Mg, Zn$ ) and  $MO_6$  ( $M = Cr, Mg, Zn$ ) polyhedra coupled with the vibrations in  $PO_4$  tetrahedra [19, 20, 23]. The absorption bands recorded in the remaining wave number range, i.e.  $490\text{--}300\text{ cm}^{-1}$ , can be ascribed to the deformation vibrations of O–M–O and O–P–O bonds in  $PO_4$  groups [19–22, 24], or they can have a combined nature [21, 23].

### New solid solution

Considering approximate values of  $Zn^{2+}$  and  $Mg^{2+}$  radii in  $MO_6$  octahedra (i.e.  $0.074$  and  $0.072\text{ nm}$ ,

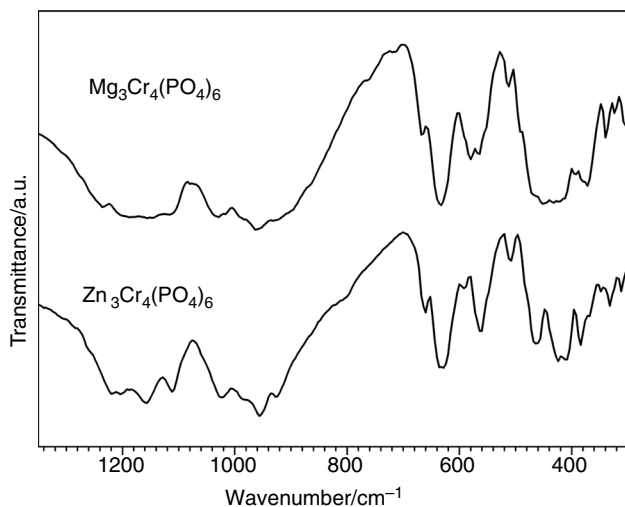
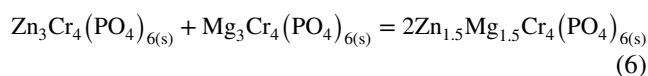


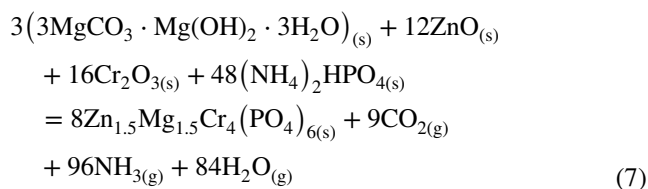
**Fig. 4** IR spectra of  $Zn_3Cr_4(PO_4)_6$  and  $Mg_3Cr_4(PO_4)_6$

respectively) [25], it can be expected that  $Zn_3Cr_4(PO_4)_6$  and  $Mg_3Cr_4(PO_4)_6$  will form a substitution solid solution. Replacement of zinc ions by magnesium ions is realized, for example, in the solid solution of the formula  $Zn_{2-x}Mg_xFeV_3O_{11}$  [26]. This type of modification is also reported in the case of pigments, for example mentioned earlier  $Mn_{3-x}Mg_xFe_4(PO_4)_6$  [9] or solid solution  $Mn_{2-x}Mg_xP_2O_7$ , which can be used as a pink pigment for conventional ceramic glazes [27].

In order to find out whether  $Zn_3Cr_4(PO_4)_6$  and  $Mg_3Cr_4(PO_4)_6$  form a solid solution, an equimolar mixture of these compounds was heated in two 12-h stages at  $1100\text{ }^\circ\text{C}$ . XRD analysis results, performed for the sample after reaction, show it to be monophasic, which indicates that a new solid solution is formed, according to the equation:



The new solid solution was obtained also according to another reaction, i.e.



The stoichiometric mixture of reactants was heated in the following stages:  $350\text{ }^\circ\text{C}(8\text{ h}) \rightarrow 550\text{ }^\circ\text{C}(8\text{ h}) \rightarrow 650\text{ }^\circ\text{C}(12\text{ h}) + 750\text{ }^\circ\text{C}(12\text{ h}) + 950\text{ }^\circ\text{C}(12\text{ h}) + 1000\text{ }^\circ\text{C}(12\text{ h}) + 1050\text{ }^\circ\text{C}(12\text{ h}) + 1100\text{ }^\circ\text{C}(12\text{ h}) \times 2$ .

The powder diffraction pattern of the sample after its last heating stage did not differ from that obtained for  $Zn_{1.5}Mg_{1.5}Cr_4(PO_4)_6$ , synthesized according to Eq. (6).

Formation of the new solid solution was corroborated by DTA method and by density measurements. On the DTA curve of  $Zn_{1.5}Mg_{1.5}Cr_4(PO_4)_6$  (Fig. 5), one endothermic effect was recorded (only its end was not registered). The effect has its onset at  $1412\text{ }^\circ\text{C}$ . Therefore, it is higher than melting temperature of  $Zn_3Cr_4(PO_4)_6$  (i.e.  $1340\text{ }^\circ\text{C}$ ) and lower than that of the estimated melting point of  $Mg_3Cr_4(PO_4)_6$  (i.e.  $\sim 1450\text{ }^\circ\text{C}$ ). Therefore, incorporation of  $Mg^{2+}$  ions into the crystal lattice of  $Zn_3Cr_4(PO_4)_6$  enhanced the thermal stability of the obtained phase. Density determined for  $Zn_{1.5}Mg_{1.5}Cr_4(PO_4)_6$  equals to  $3.84 \pm 0.01\text{ g cm}^{-3}$ , so it is between the values  $4.02$  and  $3.59\text{ g cm}^{-3}$ , determined for  $Zn_3Cr_4(PO_4)_6$  and  $Mg_3Cr_4(PO_4)_6$ , respectively. The change in density of the studied phases is consistent with the expectation; namely, it is connected with a big difference in atomic masses between zinc and magnesium.

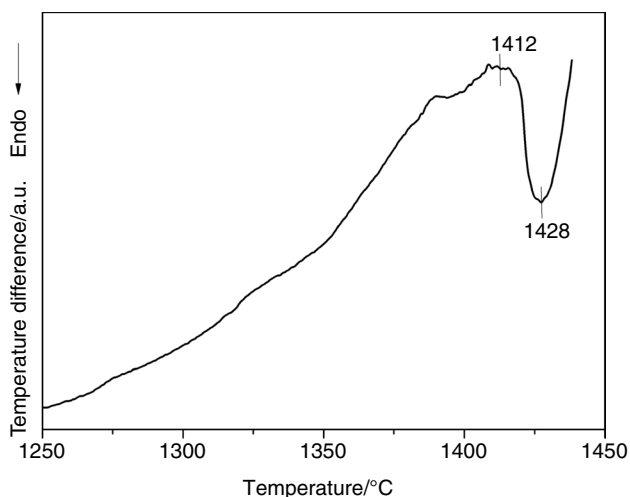


Fig. 5 Fragment of DTA curve of  $\text{Zn}_{1.5}\text{Mg}_{1.5}\text{Cr}_4(\text{PO}_4)_6$

### Spectrophotometric measurements

The monophasic samples containing  $\text{Zn}_3\text{Cr}_4(\text{PO}_4)_6$  and  $\text{Mg}_3\text{Cr}_4(\text{PO}_4)_6$  as well as the solid solution  $\text{Zn}_{3-x}\text{Mg}_x\text{Cr}_4(\text{PO}_4)_6$  for  $x = 1.50$  were subjected to UV–Vis (DRS) study that permitted estimation of the energy gaps as described inter alia in the paper [28]. Figure 6 presents the plots of  $K^2 = f(E)$ , where  $K$  is obtained from the Kubelka–Munk transformation (Spectra Analysis Program) and in the plot is marked as  $(K/M)^2$ . The energy gap values were read off as the points of intersection of the tangent to a given curve and the abscissa axis. The energy gap ( $E_g$ ) determined for  $\text{Zn}_3\text{Cr}_4(\text{PO}_4)_6$  was  $\sim 4.00$  eV, the energy gap ( $E_g$ ) determined for  $\text{Mg}_3\text{Cr}_4(\text{PO}_4)_6$  was  $\sim 3.60$  eV,

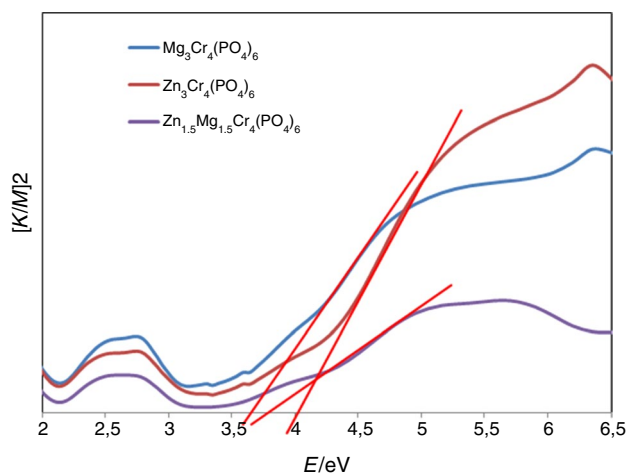


Fig. 6 Kubelka–Munk transformation of the UV–Vis–DR spectra of compounds:  $\text{Mg}_3\text{Cr}_4(\text{PO}_4)_6$ ,  $\text{Zn}_3\text{Cr}_4(\text{PO}_4)_6$  and the solid solution  $\text{Zn}_{1.5}\text{Mg}_{1.5}\text{Cr}_4(\text{PO}_4)_6$

Table 2 Chromaticity coordinates  $a^*$ ,  $b^*$ ,  $C^*$  and  $h^*$  and lightness of the resulting phases

Formula	Chromaticity coordinates			Chroma $C^*$	Lightness $L^*$
	$a^*$	$b^*$	$h^*$		
$\text{Mg}_3\text{Cr}_4(\text{PO}_4)_6$	-0.27	12.38	91.25	12.38	41.52
$\text{Zn}_{1.5}\text{Mg}_{1.5}\text{Cr}_4(\text{PO}_4)_6$	0.41	15.13	88.46	15.14	53.94
$\text{Zn}_3\text{Cr}_4(\text{PO}_4)_6$	-0.04	10.07	90.20	10.07	43.07

while the energy gap ( $E_g$ ) determined for the solid solution  $\text{Zn}_{1.5}\text{Mg}_{1.5}\text{Cr}_4(\text{PO}_4)_6$  was  $\sim 3.75$  eV. On the basis of the obtained energy gap values, the phases were classified as wide band gap semiconductors.

The physicochemical characterization of the all obtained phases was supplemented with determination of their colour expressed in the coordinates of CIE  $L^*C^*h^*$  colour space, i.e. in the system which is a variant of CIE  $L^*a^*b^*$  system. The  $L^*C^*h^*$  colour space is preferred by some industry professionals because its system correlates well with how the human eye perceives colour. In this system, the parameter  $L^*$  represents the lightness or darkness of colour as related to a neutral grey scale which is described by numbers from 0 (black) to 100 (white), the parameter  $C^*$  (chroma) represents saturation of the colour, and the parameter  $h^*$  (colour hue) represents the hue angle which characterizes the colour shade. The values of  $C^*$  and  $h^*$  are indicated by the values of  $a^*$  (the green  $\rightarrow$  red axis) and  $b^*$  (the blue  $\rightarrow$  yellow axis) parameters of CIE  $L^*a^*b^*$  system:  $C^* = (a^{*2} + b^{*2})^{0.5}$ ;  $h^* = \arctan(b^*/a^*)^{-1}$ . On the basis of the UV–Vis diffuse reflectance spectrum, the values of chromaticity coordinates  $L^* C^* h^*$  are given in Table 2. On the basis of the  $a^*$ ,  $b^*$ ,  $C^*$ ,  $h^*$  and  $L^*$  values, the colours of the obtained phases are very similar, and according to the RAL system, they can be described as boulder brown (RAL090 40 10).

### Conclusions

- For the first time, non-waste solid-state reaction method was applied to synthesize  $\text{Zn}_3\text{Cr}_4(\text{PO}_4)_6$  and  $\text{Mg}_3\text{Cr}_4(\text{PO}_4)_6$ .
- The obtained compounds of boulder brown colour have high thermal stability in air (above 1300 °C) and form crystallites of the sizes suitable for their application as inorganic pigments.
- Obtaining of a new solid solution of the formula  $\text{Zn}_{1.5}\text{Mg}_{1.5}\text{Cr}_4(\text{PO}_4)_6$  indicates the possibility of ion replacement in the crystal lattice of  $\text{Zn}_3\text{Cr}_4(\text{PO}_4)_6$  and  $\text{Mg}_3\text{Cr}_4(\text{PO}_4)_6$ . It is very important for designing of new materials, for example new inorganic pigments, because

it enables modification of composition and therefore properties of such materials.

- On the basis of the estimated energy gap values, all the phases were classified as wide band gap semiconductors.

Studies of  $Zn_3Cr_4(PO_4)_6$  and  $Mg_3Cr_4(PO_4)_6$  as well as the new solid solution  $Zn_{1.5}Mg_{1.5}Cr_4(PO_4)_6$  in the aspect of their colour properties and anticorrosion efficiency as the potential ceramic pigments are planned.

## References

- Xue X, Tang S, Yuan XY, Yue YB, Liu JK, Yang XH. One-step crushing & cladding technology and enhanced anticorrosion activity of  $Zn_3(PO_4)_2@AlH_2P_3O_{10}$  pigment. *J Alloys Compd.* 2018;744:837–48.
- Llusar M, Zielinska A, Tena MA, Badenes JA, Monrós G. Blue-violet ceramic pigments based on Co and Mg  $Co_{2-x}Mg_xP_2O_7$  diphosphates. *J Eur Ceram Soc.* 2010;30:1887–96.
- Jašková V, Kalendová A. Anticorrosive coatings containing modified phosphates. *Prog Org Coat.* 2012;75:328–34.
- Xu S, Yan X, Bu Q, Xia H. Highly efficient conversion of carbohydrates into 5-hydroxymethylfurfural using the bi-functional  $CrPO_4$  catalyst. *RSC Adv.* 2016;6:8048–52.
- Gomonaj V, Toulhoat H. Selective oxidation of methane to formaldehyde catalyzed by phosphates: kinetic description by bond strengths and specific total acidities. *ACS Catal.* 2018;8:8263–72.
- Choi C, Seo S-D, Shim H-W, Dar MA, Cho IS, Kim D-W. Facile synthesis and electroactivity of 3-D hierarchically superstructured cobalt orthophosphate for lithium-ion batteries. *J Alloys Compd.* 2015;652:100–5.
- Grub M, Glaum R. Preparation and single crystal structure refinement of mixed orthophosphates  $M_3Cr_4(PO_4)_6$  ( $M = Mg, Zn, Cu$ )—copper(II) in compressed octahedral coordination. *Z Kristallogr.* 1997;212:510–8.
- Glaum R. Beiträge zum thermischen Verhalten wasserfreier Phosphate VIII. Darstellung und Kristallstruktur von  $Cr_7(PO_4)_6$ . Das erste gemischtvalente Phosphat mit Cr(II) und Cr(III). *Z Kristallogr.* 1993;205:69–83.
- Llusar M, Badenes JA, García A, Gargori C, Galindo R, Monrós G. Solid solutions of mixed metal  $Mn_{3-x}Mg_xFe_4(PO_4)_6$  orthophosphates: colouring performance within a double-firing ceramic glaze. *Ceram Int.* 2011;37:493–504.
- Bosacka M, Blonska-Tabero A, Filipek E, Luxova J, Šulcová P. High-temperature reactions in the  $Co_3Cr_4(PO_4)_6$ - $Cr(PO_3)_3$  system. New compound  $CoCr_2(P_2O_7)_2$  and its properties. *J Therm Anal Calorim.* 2017;130:95–101.
- Gorodylova N, Šulcová P. DTA-TGA and XRD study of the formation of LISICON-type  $Li_{1+x}Cr_xZr_{2-x}(PO_4)_3$  ceramic using  $ZrOCl_2 \cdot 8H_2O$  as precursor. *J Therm Anal Calorim.* 2018;133:405–11.
- Blonska-Tabero A. A new iron lead vanadate  $Pb_2FeV_3O_{11}$ : synthesis and some properties. *Mater Res Bull.* 2009;44:1621–5.
- Walczak J, Filipek E, Tabero P.  $CrVMoO_7$  and phase equilibria in the  $V_9Mo_6O_{40}$ - $CrVMoO_7$  system. *Thermochim Acta.* 1992;206:279–84.
- Gorodylova N, Šulcová P, Bosacka M, Filipek E. DTA-TG and XRD study on the reaction between  $ZrOCl_2 \cdot 8H_2O$  and  $(NH_4)_2HPO_4$  for synthesis of  $ZrP_2O_7$ . *J Therm Anal Calorim.* 2014;118:1095–100.
- Bosacka M, Jakubus P, Rychlowska-Himmel I. Obtaining of chromium(III) phosphates(V) in the solid state and their thermal stability. *J Therm Anal Calorim.* 2007;88:133–7.
- McNally RN, Peters FI, Ribbe PH. Laboratory furnace for studies in controlled atmospheres: melting points of  $MgO$  in a  $N_2$  atmosphere and of  $Cr_2O_3$  in  $N_2$  and in air atmospheres. *J Am Ceram Soc.* 1961;44:491–3.
- Buxbaum G, Pfaff G. Industrial inorganic pigments. Weinheim: Wiley-VCH; 2005.
- Rulmont A, Cahay R, Liegeois-Duyckaerts M, Tarte P. Vibrational spectroscopy of phosphates: some general correlations between structure and spectra. *Eur J Solid State Inorg Chem.* 1991;28:207–19.
- Korchemkin IV, Pet'kov IV, Kurazhkovskaya VS, Borovikova EY. Synthesis of sodium nickel phosphate and its crystallographic spectroscopic and temperature-controlled X-ray diffraction study. *Russ J Inorg Chem.* 2015;60:265–9.
- Touaiher M, Hajbi AE. Preparation and characterisation of the compounds  $MFePO_5$  ( $M = Ni, Cu$ ). *Adv Mat Res.* 1994;1–2:215–22.
- Baran EJ, Roncaglia DI. Infra-red spectra of  $\alpha$ - $CrPO_4$ -type phases. *Spectrochim Acta.* 1988;44A:399–401.
- Bushiri MJ, Jayasree RS, Fakhfakh M, Nayar VU. Raman and infrared spectra analysis of thallium niobyl phosphates:  $Tl_2NbO_2PO_4$ ,  $Tl_3NaNb_4O_9(PO_4)_2$  and  $TlNbOP_2O_7$ . *Mater Chem Phys.* 2002;73:179–85.
- Wang X, Vander Griend DA, Stern ChL, Poepelmeier KR. Structure and cation distribution of new ternary vanadates  $FeMg_2V_3O_{11}$  and  $FeZn_2V_3O_{11}$ . *J Alloys Compd.* 2000;298:119–24.
- Stranford GT, Condrate RA. The infrared and Raman spectra of  $\beta$ - $TaPO_4$  and  $\beta$ - $NbPO_4$ . *J Mater Sci Lett.* 1984;3:303–6.
- Shannon RD. Revised effective ionic radii and systematic studies of interatomic distances in halides and chalcogenides. *Acta Crystallogr.* 1976;A32:751–67.
- Blonska-Tabero A, Filipek E, Tabero P. Synthesis and selected properties of a new solid solution in the  $Zn_2FeV_3O_{11}$ - $Mg_2FeV_3O_{11}$  system. *J Therm Anal Calorim.* 2012;109:671–6.
- Llusar M, García A, Gargori C, Galindo R, Badenes JA, Monrós G. Synthesis of diphosphate  $Mn_{2-x}Mg_xP_2O_7$  solid solutions with thortveitite structure: new pink ceramic dyes for the colouration of ceramic glazes. *J Eur Ceram Soc.* 2012;32:765–76.
- Piz M, Filipek E. Synthesis and homogeneity range of  $Yb_{8-x}Y_xV_2O_{17}$  in the  $Yb_8V_2O_{17}$ - $Y_8V_2O_{17}$  system. *J Therm Anal Calorim.* 2017;130:277–83.

**Publisher's Note** Springer Nature remains neutral with regard to jurisdictional claims in published maps and institutional affiliations.